Commun Nonlinear Sci Numer Simulat 17 (2012) 1813–1823

Contents lists available at SciVerse ScienceDirect

Commun Nonlinear Sci Numer Simulat

journal homepage: www.elsevier.com/locate/cnsns

# High-order sliding mode controller with backstepping design for aeroelastic systems

Chieh-Li Chen [a], Chao Chung Peng [a], Her-Terng Yau [b,*]

[a] Department of Aeronautics and Astronautics, National Cheng Kung University, Tainan, Taiwan
[b] Department of Electrical Engineering, National Chin-Yi University of Technology, Taichung, Taiwan

ARTICLE INFO

*Article history:*
Received 2 July 2011
Received in revised form 20 August 2011
Accepted 6 September 2011
Available online 16 September 2011

*Keywords:*
Aeroelastic system
High order sliding mode control
Limit cycle oscillation
Backstepping design

ABSTRACT

A nonlinear system for controlling flutter in an aeroelastic system is proposed. The dynamic model describes the plunge and pitch motion of a wing. Interacting nonlinear forces such as structural and aerodynamic forces cause destabilizing phenomena such as flutter and limit cycle oscillation on the wing. Aeroelastic models have a wing section with only a single trailing-edge control surface for suppressing limit cycle oscillation. When modeling a single control surface, the controller design can achieve trajectory control of either plunge displacement or pitch angle, but not both, and internal dynamics describe the residual motion in closed-loop systems. Internal dynamics of aeroelasticity depend on model parameters such as freestream velocity and spring constant. Since single control surfaces have limited effectiveness, this study used leading- and trailing-edge control surfaces to improve control of limit-cycle oscillation. Moreover, two control surfaces were used to provide sufficient flexibility to shape both the plunge and the pitch responses. In this study, high order sliding mode control (HOSMC) with backstepping design achieved system stability and eliminated limit cycle phenomenon. Compared to the conventional sliding mode control design, the proposed control law not only preserves system robustness, but also avoids chatter phenomenon. Simulation results show that the proposed controller effectively regulate the response to origin in state space even under saturated controller input.



## 1. Introduction

An aeroelastic system refers to an aircraft system in which interaction of the structure, inertia and aerodynamics cause flutter and limit cycle oscillation. The cause of limit cycle oscillation remains uncertain but is presumably a nonlinear aerodynamic effect of the structure. Tests of spring stiffness show that limit cycle oscillation results mainly from the nonlinear term, a constant deterioration of the wing structure. Therefore, an effective controller design is needed to suppress both flutter and limit cycle oscillation. Since the emergence of the robust control field in 1950, one of the most important advances has been in variable structure control, *i.e.*, sliding mode control. Essentially, the design rule states that, because a confined system must approach the origin of the sliding plane, it acquires robustness with respect to external disturbance or system uncertainty. Nevertheless, an unsolved problem is chatter resulting from high frequency switching of the system trajectory across the sliding mode due to bandwidth limitation during implementation or simulation. A sliding boundary layer usually solves the problem but at the cost of system precision. Hence, the objective of this study was to improve sliding mode control without causing chatter or loss of system precision.

The dynamics of an aeroelastic system vary with the external force exerted, *i.e.*, lift and moment, due to the effects of pitch angle and plunge displacement on the aerofoil. Numerous studies have performed experimental dynamic analyses.

* Corresponding author. Fax: +886 4 23924419.
*E-mail address:* pan1012@ms52.hinet.net (H.-T. Yau).

1007-5704/$ - see front matter © 2011 Elsevier B.V. All rights reserved.
doi:10.1016/j.cnsns.2011.09.011

For instance, a literature review by Singh and Brenner [1] applied describing function for experimentally validating plunge displacement and for frequency prediction. Lee et al. [2] showed that limit cycle oscillation is common in subsonic flight. Lee and LeBlanc [3] showed that plunge displacement caused by limit cycle oscillation increases with flight speed in the presence of a hard spring in a pitch state. A study of stable and unstable regimes by O'neill and Strganac [4] showed that the location of an elastic axis and flight speed could be used to predict limit cycle oscillation given flight speed and initial system conditions. Zhao and Yang [5] also showed that the location of a specific elastic axis may induce chaotic effects when flight speed exceeds a threshold in an elastic system such as a nonlinear spring in a pitch state. Readers are referred to Kim and Lee [6] and Price et al. [7] for additional references for system dynamics.

In addition to system dynamics, another line of research in aerolastic systems is the design of control laws that minimize flutter. Many studies have proposed control law designs in which the system is modeled as simply a trailing edge control input. A study of plunge displacement and pitch angle by Bhoir and Singh [8] showed that feedback linearization converges the system to the origin. In a study of spring stiffness by Gujjula et al. [9], both states approached zero in a proposed adaptive neural network, which demonstrated the enhanced design flexibility enabled by two control edges. Strganac et al. [10] effectively controlled limit cycle in a nonlinear adaptive manner in a system that considered the input term of the trailing edge, which resulted in a state determined by internal dynamics and system stability. To solve this problem, new aeroelastic systems with both leading and trailing edges have been developed to control both plunge displacement and pitch angle. Platanitis and Strganac [11] applied an adaptive control law design in a system with uncertainty modeled as a two control edge system. Feedback linearization effectively inhibited system flutter. Many other methods have been proposed for controlling aeroelastic systems (*e.g.* [12–16] and references therein).

Sliding mode control (SMC) is an effective alternative for controlling nonlinear systems [17]. However, conventional SMC assumes that control can be switched instantaneously from one value to another, which is impossible due to finite time delays and the practical limitations of systems. This non-ideal switching causes an undesirable phenomena called chatter. Chatter phenomenon boundary layers are generally effective for controlling nonlinear systems [18]. The backstepping approach is a nonlinear technique widely used in control design. The multiple advantages of this approach include its large set of globally and asymptotically stabilizing control laws and its capability to improve robustness and solve adaptive problems. The method uses a recursive procedure to link a selected Lyapunov function with a controller design and can suppress and synchronize nonlinear systems [19,20]. The scheme in this paper allows the controlled system to be robust to external disturbances and incorporate backstepping design processes to give the designer to easily and systematically implement the controller. Otherwise, the high order control scheme in the final step of backstepping design process can eliminate the chattering phenomenon in the control input to make it can be achieved in real physical system. However, none of the proposed methods in my surveyed papers can obtain such kind robust continuous controller for controlling flutter in an aeroelastic system. Therefore, it is necessary and important to develop the sliding mode control of aeroelastic systems using backstepping method with high order control scheme.

This work developed a strategy for use in aeroelastic systems to control unsteady phenomena such as flutter and limit cycle oscillation. The proposed input–output control scheme comprises the sliding mode controller and the backstepping feedback. The proposed method uses a high order sliding mode controller, which is introduced in the final step of the backstepping procedure, to provide a continuous input to a robust controller. Simulation results show that the proposed controller can eliminate flutter in aeroelastic systems with continuous control input.

## 2. Mathematic modeling of aeroelastic systems

An aeroelastic system describes wing dynamics in the presence of a flow field. Interacting forces between the structure, the moment of inertia and air flow destabilize aircraft by producing flutter and limit cycle oscillation [21,22]. Because flutter can eventually damage a wing structure, flutter must be shed during flight.

Fig. 1 shows an aeroelastic system model in which the wing has two degrees of freedom, *i.e.*, plunge displacement $h$ and pitch angle $\alpha$, where $\gamma$ and $\beta$ are angles of the leading and trailing edges, respectively. The wing structure includes a linear spring oriented along the plunge displacement direction, a rotational spring along the pitch angle, and corresponding dampers. Hence, in the presence of a flow field, the wing at a flight speed $U$ oscillates along the plunge displacement direction and rotates at the pitch angle about the elastic axis.

The dynamic equation for an aeroelastic system is

$$\begin{bmatrix} I_\alpha & m_w x_\alpha b \\ m_w x_\alpha b & m_t \end{bmatrix} \begin{bmatrix} \ddot{\alpha} \\ \ddot{h} \end{bmatrix} + \begin{bmatrix} c_\alpha & 0 \\ 0 & c_h \end{bmatrix} \begin{bmatrix} \dot{\alpha} \\ \dot{h} \end{bmatrix} + \begin{bmatrix} k_\alpha(\alpha) & 0 \\ 0 & k_h \end{bmatrix} \begin{bmatrix} \alpha \\ h \end{bmatrix} = \begin{bmatrix} M \\ -L \end{bmatrix} \tag{1}$$

where $m_t$ is the total weight of the main wing and supporter alike, $m_w$ is the weight of the main wing, $x_\alpha$ is the dimensionless distance between the center of mass and the elastic axis, $I_\alpha$ is the moment of inertia, $b$ is the midchord, $c_\alpha$ and $c_h$ are the damping coefficients of the pitch angle and the plunge displacement respectively, $k_h$ and $k_{\alpha(\alpha)}$ are the spring stiffness coefficients of the plunge displacement and the pitch angle respectively, and $k_{\alpha(\alpha)}$ is a nonlinear term. The nonlinear $\alpha k_{\alpha(\alpha)}$ of the spring, a hard spring in fact, which is actually a hard spring, is defined as

$$\alpha k_{\alpha(\alpha)} = k_1\alpha + k_2\alpha^3 \tag{2}$$

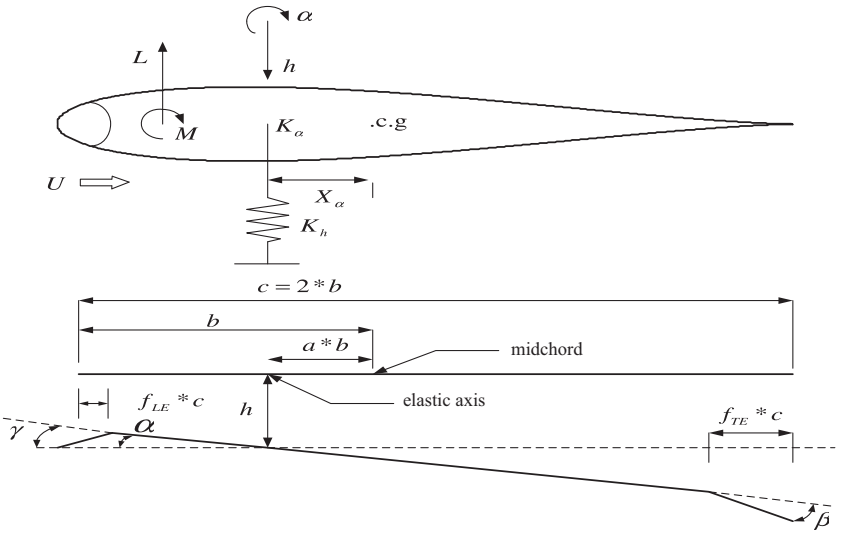


**Fig. 1.** An aeroelastic system model with two freedoms, the plunge displacement and the pitch angle.

The aerodynamic terms $L$ and $M$ (lift and moment, respectively), which are applicable in low frequency and subsonic flight, are defined as in Theodorsen and Garrick [21]:

$$L = \rho U^2 b c_{l_\alpha} s_p \left[\alpha + (\dot{h}/U + \left(\frac{1}{2} - a\right) b(\alpha/U))\right] + \rho U^2 b c_{l_\beta} s_p \beta + \rho U^2 b c_{l_\gamma} s_p \gamma \tag{3}$$

$$M = \rho U^2 b^2 c_{m_{\alpha-eff}} s_p \left[\alpha + (\dot{h}/U + \left(\frac{1}{2} - a\right) b(\alpha/U))\right] + \rho U^2 b^2 c_{m_{\beta-eff}} s_p \beta + \rho U^2 b^2 c_{m_{\gamma-eff}} s_p \gamma \tag{4}$$

where $\rho$ is air density, $U$ is the flight speed, $a$ is the dimensionless distance between the elastic axis and the mid-chord, which is a significant parameter in terms of system stability, $s_p$ is the Wind Span length, $c_{l_\alpha}$ and $c_{m_\alpha}$ are the lift coefficient and moment coefficient per unit angle of attack respectively, $c_{l_\beta}$ and $c_{m_\beta}$ are the lift coefficient and moment coefficient per unit angle respectively against the trailing edge, respectively, and $c_{l_\gamma}$ and $c_{m_\gamma}$ are the lift coefficient and moment coefficient per unit angle, respectively, against the leading edge. The $c_{m_{\alpha-eff}}$, $c_{m_{\beta-eff}}$ and $c_{m_{\gamma-eff}}$, which are the moment derivative coefficient per unit angle of attack, trailing edge and leading edge, respectively, are defined as

$$\begin{aligned} c_{m_{\alpha-eff}} &= \left(\frac{1}{2} + a\right) c_{l_\alpha} + 2c_{m_\alpha} \\ c_{m_{\beta-eff}} &= \left(\frac{1}{2} + a\right) c_{l_\beta} + 2c_{m_\beta} \\ c_{m_{\gamma-eff}} &= \left(\frac{1}{2} + a\right) c_{l_\gamma} + 2c_{m_\alpha} \end{aligned} \tag{5}$$

This study experimentally validated the model in the case of a symmetric wing structure, *i.e.*, $c_{m_\alpha} = 0$, subjected to low frequency, subsonic flight conditions.

This section describes the nonlinearity of an aeroelastic system. For convenience, the definitions used in numeric simulations of its dynamics are $c_1 = \rho U^2 b s_p$ and $c_2 = \rho U^2 b^2 s_p$, and the lift term in Eq. (3) and moment term in Eq. (4) are rewritten as

$$\begin{aligned} L &= c_1 c_{l_\alpha} \left[\alpha + \left(\dot{h}/U + \left(\frac{1}{2} - a\right) b(\alpha/U)\right)\right] + c_1 c_{l\beta} \beta + c_1 c_{l\gamma} \gamma \\ M &= c_2 c_{m_{\alpha-eff}} \left[\alpha + \left(\dot{h}/U + \left(\frac{1}{2} - a\right) b(\alpha/U)\right)\right] + c_2 c_{m_{\beta-eff}} \beta + c_2 c_{m_{\gamma-eff}} \gamma \end{aligned} \tag{6}$$

Defining the state variables as $x_1 = \alpha$, $x_2 = \dot{\alpha}$, $x_3 = h$, $x_4 = \dot{h}$ converts the dynamic equation into a state space representation:

$$\begin{aligned} \dot{x}_1 &= x_2 \\ \dot{x}_2 &= c_{\alpha_1} x_1 + c_{\alpha_{non1}} x_1^3 + c_{\dot{\alpha}_1} x_2 + c_{h_1} x_3 + c_{\dot{h}_1} x_4 + c_{\beta_1} \beta + c_{\gamma_1} \gamma \\ \dot{x}_3 &= x_4 \\ \dot{x}_4 &= c_{\alpha_2} x_1 + c_{\alpha_{non2}} x_1^3 + c_{\dot{\alpha}_2} x_2 + c_{h_2} x_3 + c_{\dot{h}_2} x_4 + c_{\beta_2} \beta + c_{\gamma_2} \gamma \end{aligned} \tag{7}$$

where parameters are defined as

$$c_{\alpha_1} = c_2 m_t c_{m_{\alpha-eff}} + c_1 m_w x_\alpha b c_{l_\alpha} - m_t k_1$$

$$c_{\alpha_{non1}} = -m_t k_2$$

$$c_{\dot{\alpha}_1} = c_2 m_t c_{m_{\alpha-eff}} \left(\frac{1}{2} - a\right) b(1/U) + c_1 m_w x_\alpha b c_{l_\alpha} \left(\frac{1}{2} - a\right) b(1/U) - c_\alpha m_t$$

$$c_{h_1} = k_h m_w x_\alpha b$$

$$c_{\dot{h}_1} = c_2 m_t c_{m_{\alpha-eff}} (1/U) + c_1 m_w x_\alpha b c_{l_\alpha} (1/U) + c_h m_w x_\alpha b$$

$$c_{\beta_1} = c_2 m_t c_{m_{\beta-eff}} + c_1 m_w x_\alpha b c_{l_\beta}$$

$$c_{\gamma_1} = c_2 m_t c_{m_{\gamma-eff}} + c_1 m_w x_\alpha b c_{l_\gamma}$$

**Table 1**
Simulation parameters for an aeroelastic system.

| | | | |
|---|---|---|---|
| $a$ | −0.6719 | $c_{m_\gamma}$ | −0.1005 |
| $b$ | 0.1905 m | $I_\alpha$ | $(m_w x_\alpha^2 b^2 + 0.009039)$ kg m$^2$ |
| $c_\alpha$ | 0.036 kg m$^2$/s | $k_\alpha$ ($\alpha$) | 12.77 + 1003$\alpha^2$ |
| $c_h$ | 27.43 kg/s | $k_h$ | 2844.4 N/m |
| $c_{l_\alpha}$ | 6.757 | $m_t$ | 15.57 kg |
| $c_{l_\beta}$ | 3.358 | $m_w$ | 4.34 kg |
| $c_{l_\gamma}$ | −0.1566 | $s_p$ | 0.5945 m |
| $c_{m_\alpha}$ | 0 | $x_\alpha$ | −(0.0998 + a) |
| $c_{m_\beta}$ | −0.6719 | $\rho$ | 1.225 kg/m$^3$ |

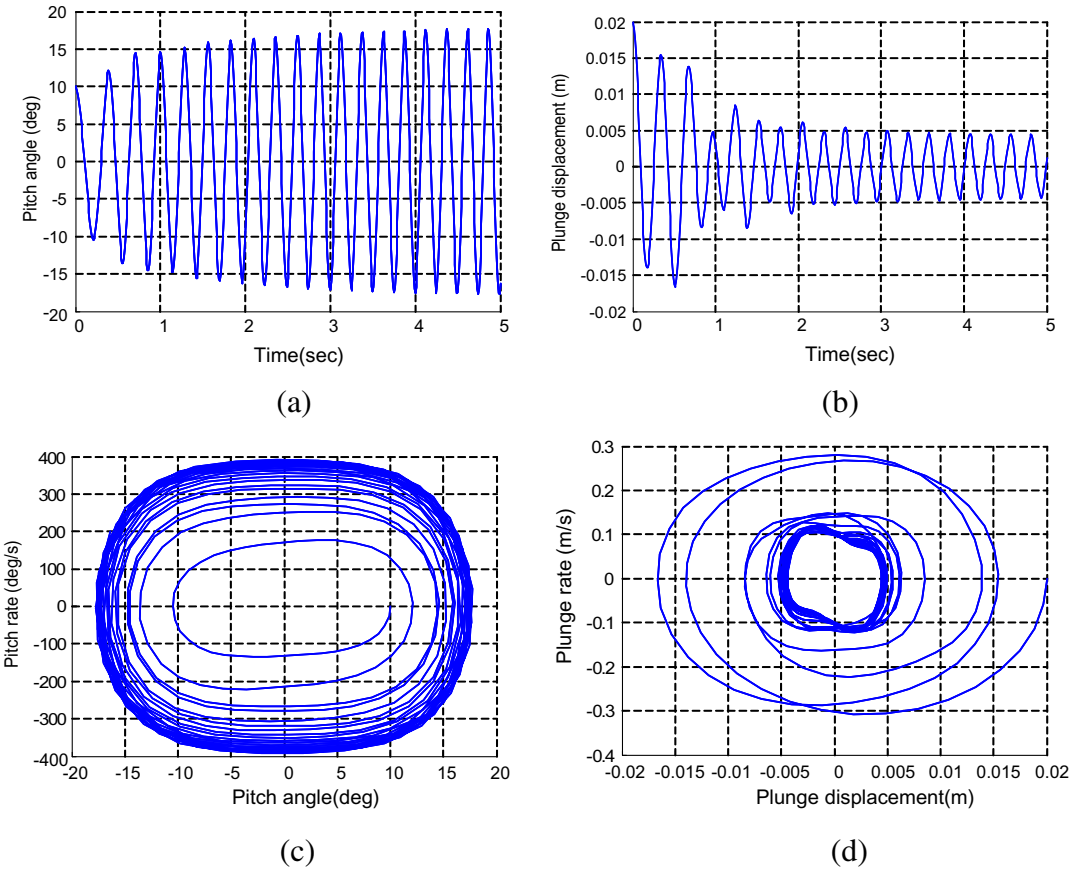


**Fig. 2.** Open loop responses of an aeroelastic system. (a) Time response of the pitch angle. (b) Time response of the plunge displacement. (c) Phase plane trajectory of the pitch angle. (d) Phase plane trajectory of the plunge displacement.

$$c_{\alpha_2} = -c_2 m_w x_\alpha b c_{m_{\alpha-eff}} - c_1 I_\alpha c_{l_\alpha} + m_w x_\alpha b k_1$$
$$c_{\alpha_{non2}} = m_w x_\alpha b k_2$$
$$c_{\dot{\alpha}_2} = -c_2 m_w x_\alpha b c_{m_{\alpha-eff}} \left(\frac{1}{2} - a\right) b(1/U) - c_1 I_\alpha c_{l_\alpha} \left(\frac{1}{2} - a\right) b(1/U) + c_\alpha m_w x_\alpha b$$
$$c_{h_2} = -k_h I_\alpha$$
$$c_{\dot{h}_2} = -c_2 m_w x_\alpha b c_{m_{\alpha-eff}} (1/U) - c_1 I_\alpha c_{l_\alpha} (1/U) - c_h I_\alpha$$
$$c_{\beta_2} = -c_2 m_w x_\alpha b c_{m_{\beta-eff}} - c_1 I_\alpha c_{l_\beta}$$
$$c_{\gamma_2} = -c_2 m_w x_\alpha b c_{m_{\gamma-eff}} - c_1 I_\alpha c_{l_\gamma}$$

Given an initial condition $x(0) = [h\ \alpha\ \dot{h}\ \dot{\alpha}] = [0.02\text{ m}\ \ 10\text{ degree}\ \ 0\text{ m/s}\ \ 0\text{ degree/s}]$ and a flight speed $U$ of 19.0625 m/s, Table 1 shows the simulated parameters, and Fig. 2 presents the simulation results.

As noted earlier, the simulations show that the long term effects of bounded limit cycle oscillation (flutter phenomenon) on the wing structure include structural fatigue and deterioration of the flight response but that short term effects are negligible. Although the cause of the limit cycle oscillation remains worthy of investigation, the literature agrees that the nonlinear contribution of the wing structure as well as the aerodynamics definitely cause limit cycle oscillation. In most simulations, such nonlinearity is modeled as a hysteresis or, alternatively, as a nonlinear term with stiffness in either pitch angle or plunge displacement.

Eq. (2) defines a nonlinear spring, *i.e.*, a hard spring, in the pitch angle. Tests show that a small value for the nonlinear parameter $k_2 < 0$ signifies a soft spring, which causes a large plunge displacement in the limit cycle oscillation. That is, parameter $k_2 = 0$ is one of many bifurcation points between system stability and instability. The parameter tuning toward system stability is hence a major concern in an aeroelastic system.

As noted above, the wing is simulated to demonstrate a repeated flutter of invariant amplitude, leading to a need to design a controller as a means to amplitude. Therefore, a controller is needed to prevent the likely damage to the wing structure. An aeroelastic state space representation, as expressed in Eq. (7) above, requires angles $\beta$ and $\gamma$, against the trailing and leading edges respectively, as control inputs for suppressing wing flutter. That is, both plunge displacement and pitch angle converge from the initial conditions toward the origin, a condition formulated as

$$x = \begin{bmatrix} \alpha \\ h \end{bmatrix} \to \begin{bmatrix} 0 \\ 0 \end{bmatrix} = x_d \tag{8}$$

This study showed how the controller design meets the stability requirement.

## 3. Backstepping design

A backsteeping design approach refers to a design technique, by use of which a complex nonlinear system is decomposed into a number of subsystems, not greater than the order of the control system. The virtual control law is then designed using the corresponding Lyapunov function associated with each individual subsystem, for the purpose of the respective Lyapunov stability in each subsystem. This design procedure is repeated and augmented until the overall system is done, that is, the entire control law is completed.

Consider a nonlinear system

$$\dot{x} = f(x) + g(x)\xi \tag{9a}$$
$$\dot{\xi} = u \tag{9b}$$

Defining $z = \xi - \alpha(x)$, then Eq. (9) turns into

$$\begin{aligned} \dot{x} &= f(x) + g(x)[\alpha(x) + z] \\ \dot{z} &= u - \frac{\partial \alpha}{\partial x}[f(x) + g(x)(\alpha(x) + z)] \end{aligned} \tag{10}$$

Defining $V_a(x, \xi) = V(x) + \frac{1}{2}[\xi - \alpha(x)]^2$ where $V(x) = \frac{1}{2}x^2$, then

$$\begin{aligned} \dot{V}_a &= \frac{\partial V}{\partial x}(f + g\alpha + gz) + z\left[u - \frac{\partial \alpha}{\partial x}(f + g(\alpha + z))\right] = \frac{\partial V}{\partial x}(f + g\alpha) + z\left[u - \frac{\partial \alpha}{\partial x}(f + g(\alpha + z)) + \frac{\partial V}{\partial x}g\right] \\ &\leqslant -W(x) + z\left[u - \frac{\partial \alpha}{\partial x}(f + g(\alpha + z)) + \frac{\partial V}{\partial x}g\right] \end{aligned} \tag{11}$$

Choosing $u = -c(\xi - \alpha(x)) - \frac{\partial \alpha(x)}{\partial x}(f(x) + g(x)\xi) - \frac{\partial V(x)}{\partial x}g(x)]$ and $c > 0$, then

$$\dot{V}_a \leqslant -W(x) - cz^2 \equiv -W_a(x, \xi) \leqslant 0 \tag{12}$$

Regarded as a control input in the above system, $\alpha(x)$ as well as $\xi$ is expected to demonstrate identical dynamics. Besides, the variable $z$ can be seen as the variance index between $\alpha(x)$ and $\xi$, and $\xi$ is expected to behave as intended through a conver-

gent $z$. The stability of Eq. (9a) is proven through $V$, and the entire system stability proof in addition to (9a) is made through $V_a$. It is essentially the fundamental idea of the backstepping design approach that the system takes specific states as the control inputs, and then the system stability is proven step by step. An insight reveals that the choice of $\alpha(x)$ is nothing short of the key to the system performance, that is, if the choice of $\alpha(x)$ makes $W(x)$ a semi-positive function, it then follows form Lasalle Theorem [23] that the system states $x$ and $\xi$ can be ensured to behave globally bounded. Yet, with a positive $W(x)$ caused by an appropriate choice of $\alpha(x)$, *i.e.* $\dot{V}_a \leqslant -W_a(x,\xi) \leqslant -W(x)$, then Lasalle–Yoshizawa Theorem [23] assures that $x = 0$ and $\xi = 0$ are the equilibrium point of the global uniformly asymptotically stable.

## 4. High order sliding mode control design

Stating the difference firstly between a high order and a conventional sliding mode controls, the advantage of such high order control is applied to a control law design. As stated in [24,25], other than the mentioned boundary layer concept, a dynamic sliding mode control is proven effectively as a way to eliminate the chattering. In most cases, a second order sliding dynamics is employed as an auxiliary system for the purpose that the dynamic system trajectory is made able to approach the origin and the system robustness is maintained. By use of an auxiliary system, it merely takes a conventional sliding mode control to reach the goal of eliminating chattering with a maintained robustness.

Just as the second order sliding mode control (SOSMC), the high order sliding mode control (HOSMC) is an issue attracting tremendous research attention in the past. As such, HOSMC is of an advantage of a conventional sliding mode control and enables itself to suppress the chattering. The HOSMC designed is illustrated with an example as follows. Consider a system

$$\dot{x} = Ax + Bu + d, \quad x \in R^n,\ u \in R,\ d \in R \tag{13}$$

A sliding plane is designed as

$$s(x,t) = Cx \tag{14}$$

Generalization of Eq. (14) induces an $r$th order sliding dynamics, *i.e.* the auxiliary system, represented as

$$\begin{aligned}
\dot{s}(x,t) &= CAx + CBu + Cd \\
\ddot{s}(x,t) &= CA^2x + CABu + CAd + CB\dot{u} + C\dot{d} \\
&\vdots \\
s^{(r)}(x,t) &= CA^r x + \sum_{m=1}^{r} CA^{m-1}Bu^{(r-m)} + \sum_{m=1}^{r} CA^{m-1}d^{(r-m)}
\end{aligned} \tag{15}$$

where $s(\cdot)^{(r)}$ represents the $r$th derivative of the sliding function. The goal is to design an input such that $s(x,t)$ together with its $(r-1)$th derivative converges to zero within a limited time frame, that is,

$$s = \dot{s} = \ddot{s} = \cdots s^{(r-1)} = 0 \tag{16}$$

On the right hand side of the last in Eq. (15) are the system input, external disturbance and a function differentiable up to $(r-1)$ order. By implication, Eq. (16) indicates the condition $CA^{m-1}B \neq 0$. In the HOSMC design, applying the control law $u^{(r-1)}$ to an integrator, a low pass filter, yields the control input $u$, a smooth control signal suitable for practical application.

## 5. Application of HOSMC to aeroelastic systems by backstepping design

It is intended in this section that an aeroelastic system is designed with a backstepping approach, and a control law is designed through a high order sliding mode control technique. For the test whether such control law maintains the robustness against the external disturbance, matched external disturbances $d_1(x,t)$ and $d_2(x,t)$ are introduced into Eq. (7) of the control system. The physical meaning of external disturbances $d_1$ and $d_2$ denote the unstructured system models and uncorrected system parameters of aeroelastic system in this study. Then letting variables $u_1 = c_{\beta_1}\beta + c_{\gamma_1}\gamma$ and $u_2 = c_{\beta_2}\beta + c_{\gamma_2}\gamma$, two sets of strict nonlinear feedback systems are represented as

$$\begin{aligned}
\dot{x}_1 &= x_2 \\
\dot{x}_2 &= c_{\alpha_1}x_1 + c_{\alpha_{non1}}x_1^3 + c_{\dot{\alpha}_1}x_2 + c_{h_1}x_3 + c_{\dot{h}_1}x_4 + u_1 + d_1
\end{aligned} \tag{17}$$

$$\begin{aligned}
\dot{x}_3 &= x_4 \\
\dot{x}_4 &= c_{\alpha_2}x_1 + c_{\alpha_{non2}}x_1^3 + c_{\dot{\alpha}_2}x_2 + c_{h_2}x_3 + c_{\dot{h}_2}x_4 + u_2 + d_2
\end{aligned} \tag{18}$$

Firstly letting $x_2$ be an independent input, there exists in Eq. (17) a state feedback control law

$$x_2 = \phi_1(x_1) = -k_1x_1 \tag{19}$$

where $k_1 > 0$. Consider the Lyapunov function $V_1 = x_1^2/2$ associated with the subsystem $x_1$

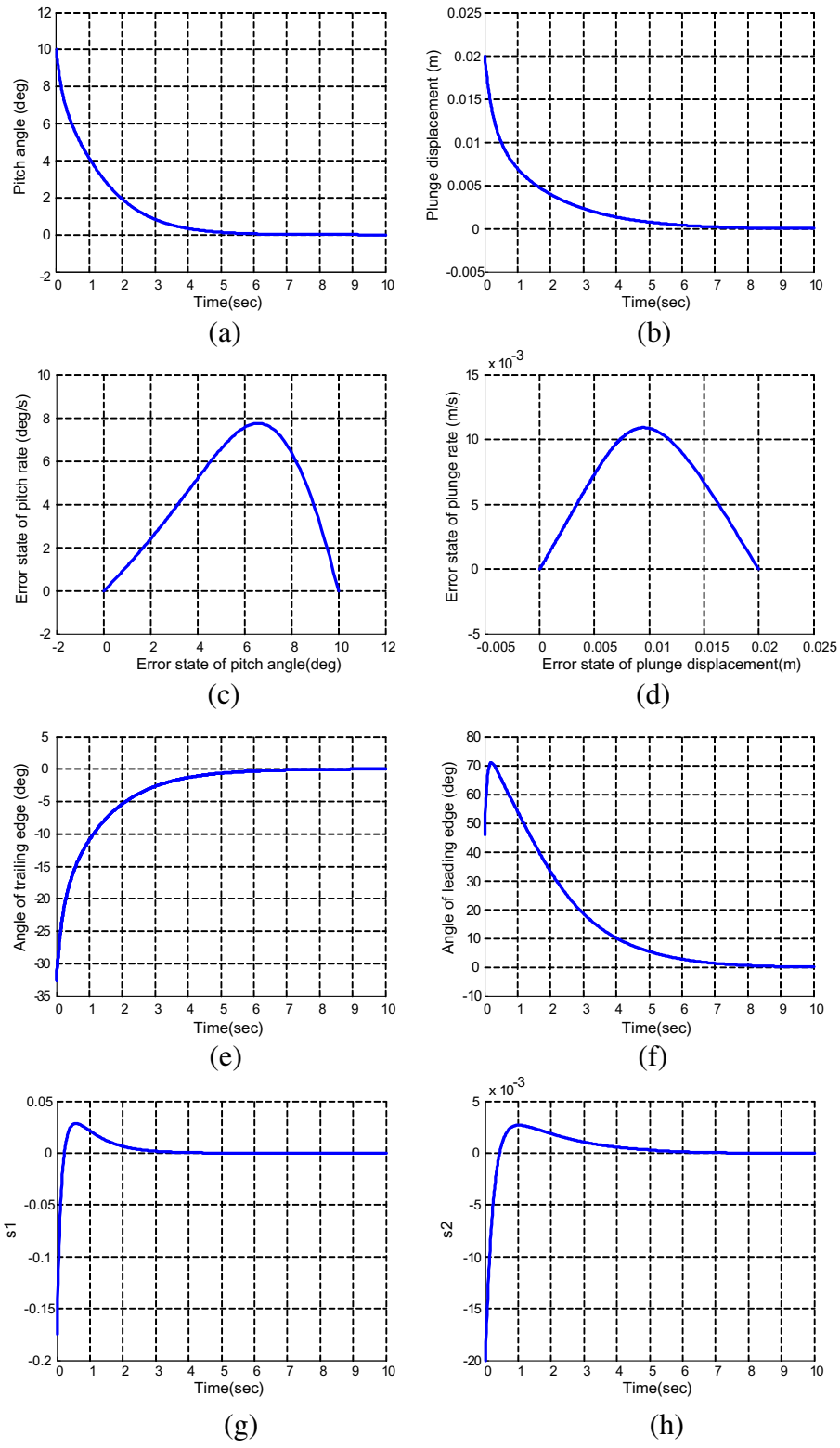


**Fig. 3.** Time responses of an unconstrained wing control in the HOSMC. (a) Time response of the pitch angle. (b) Time response of the plunge displacement. (c) Phase plane trajectory of the pitch angle. (d) Phase plane trajectory of the plunge displacement. (e) Time response of the trailing edge angle. (f) Time response of the leading edge angle. (g) Time response of the sliding plane. (h) Time response of the sliding plane.

$$\dot{V}_1 = x_1\dot{x}_1 = -k_1x_1^2 \leqslant 0 \tag{20}$$

Introducing the virtual control law $\phi_1(x_1)$ into the subsystem $x_1$, with an error function defined as $z_1 = x_2 - \phi_1(x_1)$, the subsystem $(x_1,z_1)$ is converted into

$$\begin{aligned}\dot{x}_1 &= -k_1x_1 + z_1\\ \dot{z}_1 &= c_{\alpha_1}x_1 + c_{\alpha_{non1}}x_1^3 + c_{\dot{\alpha}_1}x_2 + c_{h_1}x_3 + c_{\dot{h}_1}x_4 + u_1 - \dot{\phi}_1 + d_1\end{aligned} \tag{21}$$

The control law is chosen as

$$u_1 = -(c_{\alpha_1}x_1 + c_{\alpha_{non1}}x_1^3 + c_{\dot{\alpha}_1}x_2 + c_{h_1}x_3) + c_{\dot{h}_1}x_4 + \dot{\phi}_1 - k_2z_1 + \int_0^t v_1 d\tau \tag{22}$$

A substitution of Eq. (22) into (21) yields

$$\dot{z}_1 = -k_2z_1 + \int_0^t v_1 d\tau + d_1(t) \tag{23}$$

Letting $\dot{z}_1 = z_2$ and $[s_1\ s_2] = [z_{n-1}\ z_n]$, the auxiliary extended second order sliding dynamics is represented as

$$\begin{aligned}\dot{s}_1 &= s_2\\ \dot{s}_2 &= -k_2s_2 + v_1 + \dot{d}_1(t)\end{aligned} \tag{24}$$

Given all the states of $s_2$, an auxiliary sliding plane is chosen as

$$\sigma_1 = s_2 + k_ns_1 \tag{25}$$

Define a control law $v_1$ as a constant approaching speed

$$v_1 = -\xi_1\mathrm{sgn}(\sigma_1) \tag{26}$$

Letting a Lyapunov function be $V_{\sigma_1} = \sigma_1^2/2$, then

$$\dot{V}_{\sigma_1} = \sigma_1\dot{\sigma}_1 = \sigma_1[\dot{s}_2 + k_n\dot{s}_1] = \sigma_1[-k_ns_2 + v_1 + \dot{d}_1(t) + k_ns_2] \leqslant -|\sigma_1|[\xi_1 - \sup|\dot{d}_1(t)|] \tag{27}$$

A choice of $\xi_1 \geqslant \sup|\dot{d}_1(t)|$ ensures $\dot{V}_{\sigma_1} < 0$.

Likewise, designed for Eq. (18), $x_2$, a state feedback control law, is defined as

$$x_4 = \phi_3(x_3) = -k_3x_3 \tag{28}$$

Introducing the virtual control law $\phi_3(x_3)$ into the subsystem $x_3$, with an error function defined as $z_3 = x_4 - \phi_3(x_3)$, the subsystem $(x_3,z_3)$ is converted into

$$\begin{aligned}\dot{x}_3 &= -k_3x_3 + z_3\\ \dot{z}_3 &= c_{\alpha_2}x_1 + c_{\alpha_{non2}}x_1^3 + c_{\dot{\alpha}_2}x_2 + c_{h_2}x_3 + c_{\dot{h}_2}x_4 + u_2 - \dot{\phi}_3 + d_2\end{aligned} \tag{29}$$

The control law is chosen as

$$u_2 = -(c_{\alpha_2}x_1 + c_{\alpha_{non2}}x_1^3 + c_{\dot{\alpha}_2}x_2 + c_{h_2}x_3 + c_{\dot{h}_2}x_4) + \dot{\phi}_1 - k_3z_3 + \int_0^t v_2 d\tau \tag{30}$$

A substitution of Eq. (30) into (29) yields

$$\dot{z}_3 = -k_3z_3 + \int_0^t v_2 d\tau + d_2(t) \tag{31}$$

Letting $\dot{z}_3 = z_4$ and $[s_3\ s_4] = [z_3\ z_4]$, the auxiliary extended second order sliding dynamics is represented as

$$\begin{aligned}\dot{s}_3 &= s_4\\ \dot{s}_4 &= -k_3s_4 + v_2 + \dot{d}_2(t)\end{aligned} \tag{32}$$

Given all the states of $s_4$, an auxiliary sliding plane is chosen as

$$\sigma_2 = s_4 + k_ms_3 \tag{33}$$

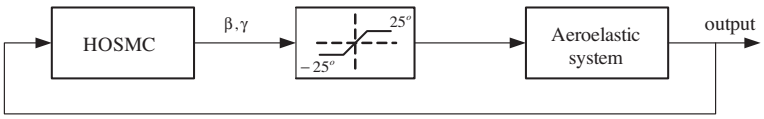


**Fig. 4.** A block diagram of the wing constrained within [−25°,25°] in the HOSMC.

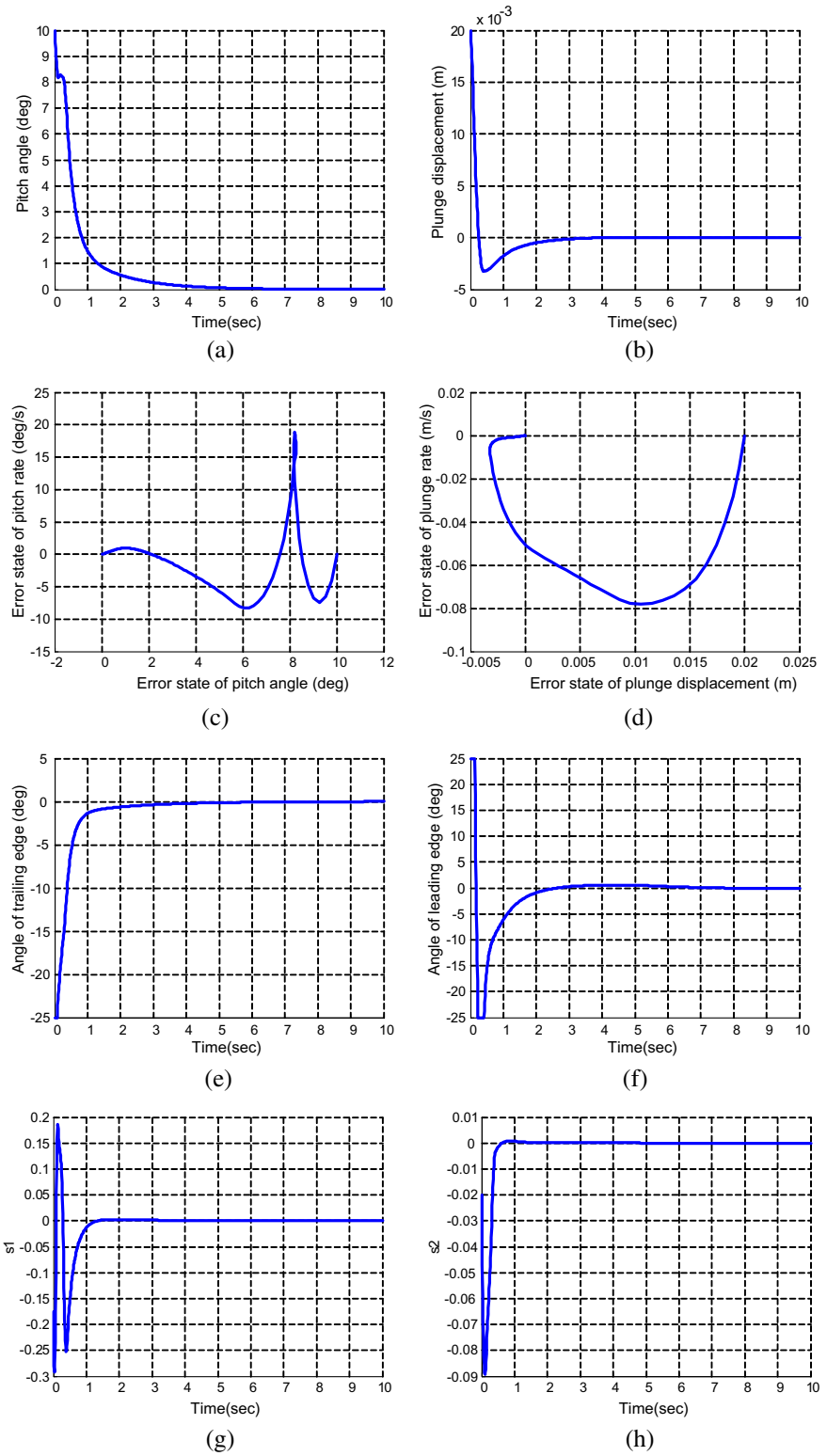


**Fig. 5.** Time responses of a wing constrained between $[-25°, 25°]$ in the HOSMC. (a) Time response of the pitch angle. (b) Time response of the plunge displacement. (c) Phase plane trajectory of the pitch angle. (d) Phase plane trajectory of the plunge displacement. (e) Time response of the trailing edge angle. (f) Time response of the leading edge angle. (g) Time response of the sliding plane. (h) Time response of the sliding plane.

Define a control law $v_2$ as a constant approaching speed

$$v_2 = -\xi_2 \ \mathrm{sgn}(\sigma_2) \tag{34}$$

Letting a Lyapunov function be $V_{\sigma_2} = \sigma_2^2/2$, then

$$\dot{V}_{\sigma_2} = \sigma_2\dot{\sigma}_2 = \sigma_2[\dot{s}_4 + k_m\dot{s}_3] = \sigma_3[-k_m s_4 + v_2 + \dot{d}_1(t) + k_m s_4] \leqslant -|\sigma_3|[\xi_2 - \sup|\dot{d}_2(t)|] \tag{35}$$

A choice of $\xi_2 \geqslant \sup|\dot{d}_2(t)|$ ensures $\dot{V}_{\sigma_2} < 0$. Therefore, it can be summarized as a theorem in the follows from the above derivation.

**Theorem 1.** *Consider the closed-loop system equations (17), (18), (22), and (30). Suppose that $h_d$ and $\alpha_d$ are bounded and smooth trajectories converging to zero, and the zero dynamics of the system are stable. Then the time responses of Eq. (1) beginning from any initial condition $x(0) = [h \ \alpha \ \dot{h} \ \dot{\alpha}] \in R^4$ tends to the origin as $t \to \infty$.*

**Proof.** A proof is shown in the above derivation. □

Following the completion of the design procedure, choosing the simulation parameters as $k_1 = 1$, $k_2 = 3$, $k_3 = 1$, $k_4 = 3$, $k_m = 3$, $k_n = 3$, $\xi_1 = 0.05$, $\xi_2 = 0.01$, the simulation results will be discussed in full in following section.

## 6. Simulation results

This section describes the numerical simulations performed to validate the above control law design. The aeroelastic system parameters (Table 1) in a HOSMC by backstepping design are simulated under the following initial conditions: $x(0) = [h \ \alpha \ \dot{h} \ \dot{\alpha}] = [0.02\ \mathrm{m} \ \ 10\ \mathrm{degree} \ \ 0\ \mathrm{m/s} \ \ 0\ \mathrm{degree/s}]$, flight speed $U$ of 19.0625 m/s, and the choice between $\xi_1 = 0.05$ and $\xi_2 = 0.01$ with references $h_d = 0$ and $\alpha_d = 0$ respectively.

Given external disturbances $d_1 = 0.01\sin(t)$ and $d_2 = 0.002\sin(t)$, Fig. 3 plots the simulations for unconstrained wing control. Figs. 3(a) and (b) are the pitch angle and plunge displacement states, respectively, at which the control law approaches the origin at Time = 4 s. It then moves toward the origin at a slower pace, which is an advantage over the preceding HOSMC in terms of the time response. However, the penalty is the increased control inputs, *i.e.*, the trailing and leading edge angles (Figs. 3(e) and (f), respectively) causing increased wing actuator deterioration. Thus, the choice of control law to meet the system performance requirement involves a tradeoff. In the presence of external disturbance, system robustness is ensured by the control law, which confines both pitch angle and plunge displacement to the vicinity of the origin.

As noted above, constraints are imposed on the controlled edge angles during the flight. Fig. 4 shows an HOSMC design with controlled edge angles confined between ±25° used as the input to the aeroelastic system through a saturation function. Fig. 5 shows the simulation results given identical initial conditions and simulation parameters. Fig. 5 shows the time responses of the wing controlled in a high order sliding mode with the angle confined to ±25°. In contrast with Figs. 3(a) and (b), Figs. 5(a) and (b) indicate that the pitch angle and the plunge displacement cannot converge to the origin exclusive of a short period of over/under shooting. Figs. 5(e) and (f) clearly show that both edges are confined as expected between ±25° during the transient response and do not approach zero until the steady state. The aeroelasticity maintains system stability by suppressing external disturbance at the expense of a small amplitude oscillation in the steady state of both edge angles.

## 7. Conclusions

This work considered the performance of an aeroelastic system in which both controlled edges are inputs. The model showed that, in a spring with nonlinear stiffness, limit cycle oscillation causes fatigue in the wing structure due to long term vibration at a constant amplitude and at an invariant frequency. Thus, HOSMC is proposed for suppressing limit cycle oscillation with a backstepping design. In terms of sliding mode control design, the main drawback is the chatter produced when switching between functions. This work proposes a derivative input term to differentiate the original sliding function in the high order sliding mode control designed by a backstepping technique. That is, the derivative term directly differentiates the input term in the dynamic sliding mode control. Simulations then confirmed that the control law designs for the derivative terms of the inputs in sliding mode effectively eliminate chatter and suppress limit cycle oscillation in wing structures.

## Acknowledgement

The financial support of this research by National Science Council, Taiwan, under the Grant No. NSC 98-2221-E-006-209-MY2 is greatly appreciated.

## References

[1] Singh SN, Brenner M. Limit cycle oscillation and orbital stability in aeroelastic systems with torsional nonlinearity. Nonlinear Dyn 2003;31:435–50.
[2] Lee BHK, Price SJ, Wong YS. Nonlinear aeroelastic analysis of airfoils: bifurcation and chaos. Prog Aerosp Sci 1999;35:205–334.

[3] Lee, BHK, LeBlanc P. Flutter analysis of a two-dimensional airfoil with cubic nonlinear restoring force. National Aeronautical Establishment, Aeronautical Note 36, National Reserch Counsil (Canada), 35438, Ottawa, PQ, Canada; 1986.
[4] O"Neill T, Strganac TW. Aeroelastic response of a rigid wing supported by nonlinear spring. J Aircraft 1998;35(4):616–22.
[5] Zhao LC, Yang ZC. Chaotic motions of an airfoil with nonlinear stiffness in incompressible flow. J Sound Vib 1990;128(2):245–54.
[6] Kim SH, Lee I. Aeroelastic analysis of a flexible airfoil with a freeplay nonlinearity. J Sound Vib 1996;193:823–46.
[7] Price SJ, Alighanbari H, Lee BHK. The aeroelastic response of a two-dimensional airfoil with bilinear and cubic nonlinearities. J Fluids Struct 1995;9:175–93.
[8] Bhoir NG, Singh SN. Output feedback nonlinear control of an aeroelastic with unsteady aerodynamics. Aerosp Sci Technol 2004;8:195–205.
[9] Gujjula S, Singh SN, Yim W. Adaptive and neural control of a wing section using leading- and trailing-edge surfaces. Aerosp Sci Technol 2005;9:161–71.
[10] Strganac TW, Ko J, Thompson DE. Identification and control of limit cycle oscillations in aeroelastic systems. J Guid Control Dynam 2000;23(6):1127–33.
[11] Platanitis G, Strganac TW. Control of a nonlinear wing section using leading- and trailing-edge surfaces. J Guid Control Dynam 2004;27(1):52–8.
[12] Ko J, Kurdila AJ, Strganac TW. Nonlinear control of a prototypical wing section with torsional nonlinearity. J Guid Control Dynam 1997;20(6):1181–9.
[13] Ko J, Strganac TW, Kurdila AJ. Stability and control of a structurally nonlinear aeroelastic system. J Guid Control Dynam 1998;21(5):718–25.
[14] Block J, Strganac TW. Applied active control for nonlinear aeroelastic structure. J Guid Control Dynam 1998;21(6):838–45.
[15] Bhoir NG, Singh SN. Control of unsteady aeroelastic system via state-dependent Riccati equation method. J Guid Control Dynam 2005;28(1):78–84.
[16] Chen MS, Chen CH, Yang FY. An-LTR-observer-based dynamic sliding mode control for chattering reduction. Automatica 2007;43(6):1111–6.
[17] Utkin VI. Sliding mode and their applications in variable structure systems, Mir Editors, Moscow, 1978.
[18] Yau HT, Lin JS, Yan JJ. Synchronization control for a class of chaotic systems with uncertainties. Int J Bifur Chaos 2005;15(7):2235–46.
[19] Wang CC, Pai NS, Yau HT. Chaos control in AFM system using sliding mode control by backstepping design. Communications in Nonlinear Science and Numerical Simulation 2010;15(3):741–51.
[20] Chen CL, Yau HT, Peng CC. Design of extended backstepping sliding mode controller for uncertain chaotic systems. Int J Nonlinear Sci Numer Simulat 2007;8(2):137–45.
[21] Theodorsen T, Garrick IE. Mechanism of flutter: a theoretical and experiment investigation of the flutter problem. NACA Rept. 685, 1940.
[22] Fung YC. An introduction to the theory of aeroelasticty. New York: Wiley; 1955.
[23] Slotine JE, Li W. Applied nonlinear control. Englewood Cliffs, New Jersey: Prentice-Hall; 1991.
[24] Aguilar LR, Martinez GR, Puebla H, Hernadez SR. High order sliding-mode dynamic control for chaotic intracellular calcium oscillations. Nonlinear Anal B: Real World Appl 2010;11:217–31.
[25] Xing WH, Singh SH. Adaptive output feedback control of a nonlinear aeroelastic structure. J Guid Control Dynam 2000;23(6):1109–16.